

# Unified position-dependent photon-number quantization in layered structures

Mikko Partanen, Teppo Häyrynen, Jani Oksanen, and Jukka Tulkki

*Department of Biomedical Engineering and Computational Science,*

*Aalto University, P.O. Box 12200, 00076 Aalto, Finland*

(Dated: March 3, 2022)

We have recently developed a position-dependent quantization scheme for describing the ladder and effective photon-number operators associated with the electric field to analyze quantum optical energy transfer in lossy and dispersive dielectrics [Phys. Rev. A, 89, 033831 (2014)]. While having a simple connection to the thermal balance of the system, these operators only described the electric field and its coupling to lossy dielectric bodies. Here we extend this field quantization scheme to include the magnetic field and thus to enable description of the total electromagnetic field and discuss conceptual measurement schemes to verify the predictions. In addition to conveniently describing the formation of thermal balance, the generalized approach allows modeling of the electromagnetic pressure and Casimir forces. We apply the formalism to study the local steady state field temperature distributions and electromagnetic force density in cavities with cavity walls at different temperatures. The calculated local electric and magnetic field temperatures exhibit oscillations that depend on the position as well as the photon energy. However, the effective photon number and field temperature associated with the total electromagnetic field is always position-independent in lossless media. Furthermore, we show that the direction of the electromagnetic force varies as a function of frequency, position, and material thickness.

## I. INTRODUCTION

The quantum optical processes and field quantization in lossy structures exhibiting interference represent a fascinating challenge to our understanding of wave-particle dualism, intertwined electric and magnetic fields, and wave-matter interactions. The quantization of the electromagnetic (EM) field in a dielectric medium has been widely studied during the last few decades especially in layered structures [1–6]. It has been established that the field operators obey the well-known canonical commutation relations [4, 5], but there are reported anomalies in the commutation relations of the intracavity ladder operators [7–11] leading to difficulties in defining a well-behaving photon number. We have recently introduced photon ladder operators associated with the electric field in a way that is consistent with the canonical commutation relations and gives further insight on the local effective photon number, thermal balance, and the formation of the local thermal equilibrium [12, 13]. This approach, however, neglects the magnetic contributions that are important in determining the properties of the total EM field, its energy density, and EM pressure.

In this paper, we extend our ladder operator formalism to describe also the magnetic field and the total EM field in layered structures. We present the photon ladder and number operators for the electric and magnetic fields and express the photon number of the total EM field in terms of the electric and magnetic photon-number operators. The electric and magnetic field associated effective photon numbers generally oscillate even in the vacuum, but we show that the oscillations balance each other so that the photon number associated with the total EM field is constant in the vacuum as expected. We also establish the relation of the local photon-number operators to the field temperatures, EM pressures, and thermal

balance of the system providing insight on the physical interpretation of the quantities. This is followed by applying the presented theoretical concepts to study the position and photon energy dependence of the effective electric, magnetic, and total EM field temperatures and corresponding local densities of states (LDOS) in a geometry of a vacuum cavity formed between two semi-infinite thermal reservoir media at different temperatures. In addition, the relation of the effective photon number to the EM pressure is studied by examining the force exerted on lossy and lossless material slabs placed inside the vacuum cavity.

## II. FIELD QUANTIZATION

### A. Noise operator formalism

The theoretical foundations of the present work originate from the noise operator formalism developed by Matloob *et al.* [5, 6]. In the noise operator formalism, the field operators are expressed in terms of the Green's function  $G(x, \omega, x')$  of the Helmholtz equation and the bosonic source field operator  $\hat{f}(x, \omega)$  obeying  $[\hat{f}(x, \omega), \hat{f}^\dagger(x', \omega')] = \delta(x - x')\delta(\omega - \omega')$  describing the material state. For example, the equation for the positive frequency part of the vector potential operator is given by  $\hat{A}^+(x, \omega) = \int_{-\infty}^{\infty} G_A(x, \omega, x') \hat{f}(x', \omega) dx'$ , where  $G_A(x, \omega, x') = \mu_0 j_0(x', \omega) G(x, \omega, x')$ , in which  $j_0(x, \omega) = \sqrt{4\pi\hbar\omega^2\epsilon_0 \text{Im}[n(x, \omega)^2]/S}$  is a scaling factor,  $n(x, \omega)$  is the refractive index of the medium,  $\hbar$  is the reduced Planck's constant,  $\epsilon_0$  is the permittivity of vacuum,  $\mu_0$  is the permeability of vacuum, and  $S$  is the area of quantization in the  $y$ - $z$  plane [5]. Similar expressions are valid for electric and magnetic field operators  $\hat{E}^+(x, \omega)$  and  $\hat{B}^+(x, \omega)$  with  $G_A(x, \omega, x')$  replaced by  $G_E(x, \omega, x') = i\omega\mu_0 j_0(x', \omega) G(x, \omega, x')$  and  $G_B(x, \omega, x') = \mu_0 j_0(x', \omega) \partial G(x, \omega, x')/\partial x$  as defined in Ref. [12].

## B. Photon operators

In any quantum electrodynamics (QED) description, the canonical commutation relations are satisfied for field quantities, i.e.,  $[\hat{A}(x, t), \hat{E}(x', t)] = -i\hbar/(\varepsilon_0 S)\delta(x - x')$  [14], but the same is not generally true for the canonical commutation relations of the ladder operators. The dominant approach in evaluating the ladder operators has been to separate the field operators obtained from QED either into the left and right propagating normal modes or into the normal modes related to the left and right inputs and the corresponding ladder operators [8, 10, 15]. This is tempting in view of the analogy with classical EM, but in most cases results in ladder operators that are not unambiguously determined due to the possibility to scale the normal modes nearly arbitrarily. Also other definitions based on separately accounting for the noise contribution have been reported [11], but they do not result in the canonical commutation relations for the ladder operators either.

We have very recently presented a quantization scheme that uses the requirement of preservation of the canonical commutation relation  $[\hat{a}(x, \omega), \hat{a}^\dagger(x', \omega')] = \delta(\omega - \omega')$  as a starting point for defining the photon annihilation operator that describes the electric field [12, 13]. In the developed formalism the electric field annihilation operator is given by [13]

$$\begin{aligned}\hat{a}_e(x, \omega) &= \sqrt{\frac{\varepsilon_0}{2\pi^2\hbar\omega\rho_e(x, \omega)}}\hat{E}^+(x, \omega) \\ &= \sqrt{\frac{\varepsilon_0}{2\pi^2\hbar\omega\rho_e(x, \omega)}}\int_{-\infty}^{\infty} G_E(x, \omega, x')\hat{f}(x', \omega)dx',\end{aligned}\quad (1)$$

where the factor  $\rho_e(x, \omega)$  has been shown to correspond to the conventional definition of the electric contribution of the local density of EM states (electric LDOS) defined as [16]

$$\begin{aligned}\rho_e(x, \omega) &= \frac{\varepsilon_0}{2\pi^2\hbar\omega}\int_{-\infty}^{\infty} |G_E(x, \omega, x')|^2 dx' \\ &= \frac{2\omega^3}{\pi c^4 S}\int_{-\infty}^{\infty} \text{Im}[n(x', \omega)^2]|G(x, \omega, x')|^2 dx' \\ &= \frac{2\omega}{\pi c^2 S}\text{Im}[G(x, \omega, x)],\end{aligned}\quad (2)$$

where  $c$  is the speed of light in vacuum.

In this work, we unify the previously introduced electric-field-based photon-number picture to the description of the total EM field. For this purpose, we first define a magnetic field annihilation operator proportional to the magnetic field operator written for positive frequencies as  $\hat{B}^+(x, \omega) = C(x, \omega)\hat{a}_m(x, \omega)$ . Just like in the case of the electric field [12], the normalization coefficient  $C(x, \omega)$  is defined by using the requirement that the canonical commutation relation is fulfilled leading to

the relation,

$$\begin{aligned}\hat{a}_m(x, \omega) &= \sqrt{\frac{\varepsilon_0 c^2}{2\pi^2\hbar\omega\rho_m(x, \omega)}}\hat{B}^+(x, \omega) \\ &= \sqrt{\frac{\varepsilon_0 c^2}{2\pi^2\hbar\omega\rho_m(x, \omega)}}\int_{-\infty}^{\infty} G_B(x, \omega, x')\hat{f}(x', \omega)dx'.\end{aligned}\quad (3)$$

In Eq. (3), the magnetic contribution of the local density of EM states (magnetic LDOS) is given by

$$\begin{aligned}\rho_m(x, \omega) &= \frac{\varepsilon_0 c^2}{2\pi^2\hbar\omega}\int_{-\infty}^{\infty} |G_B(x, \omega, x')|^2 dx' \\ &= \frac{2\omega^3}{\pi c^4 S}\int_{-\infty}^{\infty} \text{Im}[n(x', \omega)^2]\left|\frac{\partial G(x, \omega, x')}{k_0 \partial x}\right|^2 dx' \\ &= \frac{2\omega}{\pi c^2 S}\text{Im}[n(x, \omega)^2 G_{\{-r\}}(x, \omega, x)],\end{aligned}\quad (4)$$

where  $k_0 = \omega/c$  and  $G_{\{-r\}}(x, \omega, x')$  has been defined as an auxiliary Green's function calculated for a structure where all reflection coefficients have been transformed by  $r(\omega) \rightarrow -r(\omega)$ . The transformation enables writing the magnetic LDOS expression in a form resembling the electric LDOS. In homogeneous media, the electric and magnetic field annihilation operators are identical, but generally the annihilation operator for the magnetic field is different from the annihilation operator for the electric field due to different spatial dependence of electric and magnetic fields as seen from the definitions of  $G_E(x, \omega, x')$  and  $G_B(x, \omega, x')$ .

The electric and magnetic photon-number operators are obtained from the ladder operators as  $\hat{n}_i(x, \omega) = \int \hat{a}_i^\dagger(x, \omega)\hat{a}_i(x, \omega')d\omega'$ ,  $i \in \{e, m\}$ , and, therefore, their expectation values are given in terms of the Green's functions and the source field photon-number operator as

$$\begin{aligned}\langle \hat{n}_e(x, \omega) \rangle &= \frac{\varepsilon_0}{2\pi^2\hbar\omega\rho_e(x, \omega)}\int_{-\infty}^{\infty} |G_E(x, \omega, x')|^2 \langle \hat{\eta}(x', \omega) \rangle dx' \\ &= \frac{2\omega^3}{\pi c^4 S\rho_e(x, \omega)}\int_{-\infty}^{\infty} \text{Im}[n(x', \omega)^2]|G(x, \omega, x')|^2 \\ &\quad \times \langle \hat{\eta}(x', \omega) \rangle dx',\end{aligned}\quad (5)$$

$$\begin{aligned}\langle \hat{n}_m(x, \omega) \rangle &= \frac{\varepsilon_0 c^2}{2\pi^2\hbar\omega\rho_m(x, \omega)}\int_{-\infty}^{\infty} |G_B(x, \omega, x')|^2 \langle \hat{\eta}(x', \omega) \rangle dx' \\ &= \frac{2\omega^3}{\pi c^4 S\rho_m(x, \omega)}\int_{-\infty}^{\infty} \text{Im}[n(x', \omega)^2]\left|\frac{\partial G(x, \omega, x')}{k_0 \partial x}\right|^2 \\ &\quad \times \langle \hat{\eta}(x', \omega) \rangle dx',\end{aligned}\quad (6)$$

where we have defined the source field photon-number operator as  $\hat{\eta}(x, \omega) = \int \hat{f}^\dagger(x, \omega)\hat{f}(x', \omega')dx'd\omega'$  and assumed that the noise operators at different positions and at different frequencies are uncorrelated. For media in local thermal equilibrium, the source field photon-number expectation value at position  $x$  is

$$\langle \hat{\eta}(x, \omega) \rangle = \frac{1}{e^{\hbar\omega/(k_B T(x))} - 1},\quad (7)$$

where  $k_B$  is the Boltzmann constant and  $T(x)$  is the temperature distribution of the medium.

The expectation value of the total photon-number operator describing the energy quanta of the total EM field is obtained either by using a similar quantization scheme as for electric and magnetic fields or directly written as an LDOS weighted sum of the electric and magnetic photon numbers as

$$\begin{aligned} \langle \hat{n}_{\text{tot}}(x, \omega) \rangle &= \frac{|n(x, \omega)|^2 \rho_e(x, \omega) \langle \hat{n}_e(x, \omega) \rangle + \rho_m(x, \omega) \langle \hat{n}_m(x, \omega) \rangle}{|n(x, \omega)|^2 \rho_e(x, \omega) + \rho_m(x, \omega)} \\ &= \frac{\omega^3 |n(x, \omega)|^2}{\pi c^4 S \rho_{\text{tot}}(x, \omega)} \int_{-\infty}^{\infty} \text{Im}[n(x', \omega)^2] \left( |G(x, \omega, x')|^2 \right. \\ &\quad \left. + \left| \frac{\partial G(x, \omega, x')}{k(x, \omega) \partial x} \right|^2 \right) \langle \hat{\eta}(x', \omega) \rangle dx', \end{aligned} \quad (8)$$

where  $k(x, \omega) = \omega n(x, \omega)/c$  and the total EM LDOS is the sum of the electric and magnetic contributions in Eqs. (2) and (4) given by

$$\begin{aligned} \rho_{\text{tot}}(x, \omega) &= \frac{\omega^3 |n(x, \omega)|^2}{\pi c^4 S} \int_{-\infty}^{\infty} \text{Im}[n(x', \omega)^2] \\ &\quad \times \left( |G(x, \omega, x')|^2 + \left| \frac{\partial G(x, \omega, x')}{k(x, \omega) \partial x} \right|^2 \right) dx'. \end{aligned} \quad (9)$$

The total field photon number in Eq. (8) will be shown to be related to the total field energy and EM pressure providing a meaningful definition for the photon number of the total EM field. In contrast to the corresponding electric quantities, the above total EM LDOS and the photon-number expectation value are always constant in lossless media, as can be easily shown by calculating the derivatives  $\partial \rho_{\text{tot}}(x, \omega)/\partial x$  and  $\partial \langle \hat{n}_{\text{tot}}(x, \omega) \rangle / \partial x$ , which are equal to zero when the nonhomogeneous Helmholtz equation is fulfilled and the refractive index at position  $x$  is  $n(x, \omega) = 1$ . In the case of thermal fields, the photon-number operators in Eqs. (5), (6), and (8) also allow one to calculate effective local electric, magnetic, and total field temperatures as

$$T_i(x, \omega) = \frac{\hbar \omega}{k_B \ln[1 + 1/\langle \hat{n}_i(x, \omega) \rangle]}, \quad i \in \{e, m, \text{tot}\}. \quad (10)$$

### C. Thermal balance

A particularly insightful view of the electric field photon number is provided by its connection to local thermal balance between the field and matter [12]. The spectral net emission rate can be compactly written as a product of the electric LDOS and the difference of the local source field photon number and the electric field photon number as [12]

$$\langle Q(x, t) \rangle_{\omega} = \hbar \omega^2 \text{Im}[n(x, \omega)^2] \rho_e(x, \omega) [\langle \hat{\eta}(x, \omega) \rangle - \langle \hat{n}_e(x, \omega) \rangle]. \quad (11)$$

In resonant systems where the energy exchange is dominated by a narrow frequency band, condition  $\langle \hat{Q}(x, \omega) \rangle_{\omega} = 0$  can be used to approximately determine the steady-state temperature of a weakly interacting resonant particle [17]. This suggests that the electric field temperature is experimentally measurable by measuring the steady-state temperature reached by a detector with a weak field-matter interaction that is dominated by the coupling to the electric field. Similar temperature measurement setup to measure the magnetic field photon number is expected to be also possible using materials whose field-matter interactions have been engineered to be sensitive to magnetic fields instead of electric fields, using, e.g., micro-coil sensors [18] or magnetic metamaterials [19] at least at microwave frequencies. Another possible measurement setup for the local electric field temperature could, for example, use the transparent intracavity photodetector studied by Lazar *et al.* [20, 21]. Measuring the electric field at equilibrium conditions using a movable transparent intracavity detector allows one to determine the electric LDOS since the photon number is known and constant. Then changing the cavity wall temperatures and using the determined LDOS allows one to calculate the position-dependent photon number from the measured field. Measuring the magnetic field by using a similar scheme is not straightforward at optical frequencies, but the existence of the predicted phenomena could be demonstrated at microwave frequencies by using micro-coil sensors that practically do not disturb the measured magnetic field [18]. The electric and magnetic field LDOSs and photon numbers together also determine the total EM field quantities.

### D. Energy density and EM pressure

Despite its natural connection to the energy balance, the photon-number operator related to the electric field can exhibit oscillatory behavior, e.g., in vacuum cavities [12, 13]. The total photon-number operator presented in Eq. (8) does not share the same peculiarity as it accounts for both the electric and magnetic contributions, which balance out the oscillations. To further study the physical significance of the total field photon number, we will next discuss the energy density associated with the electric and magnetic contributions, and their relation to the total energy density and EM pressure.

The electric and magnetic field fluctuations and the total energy density  $\langle \hat{u}(x, t) \rangle_{\omega} = \varepsilon_0 |n(x, \omega)|^2 \langle \hat{E}(x, t) \rangle_{\omega} / 2 + \langle \hat{B}(x, t) \rangle_{\omega} / (2\mu_0)$  for a single polarization and angular frequency  $\omega$  in terms of the position-dependent photon-number operators are given by

$$\langle \hat{E}(x, t)^2 \rangle_{\omega} = \frac{\hbar \omega}{\varepsilon_0} \rho_e(x, \omega) \left( \langle \hat{n}_e(x, \omega) \rangle + \frac{1}{2} \right), \quad (12)$$

$$\langle \hat{B}(x, t)^2 \rangle_{\omega} = \frac{\hbar \omega}{\varepsilon_0 c^2} \rho_m(x, \omega) \left( \langle \hat{n}_m(x, \omega) \rangle + \frac{1}{2} \right), \quad (13)$$

$$\langle \hat{u}(x, t) \rangle_{\omega} = \hbar \omega \rho_{\text{tot}}(x, \omega) \left( \langle \hat{n}_{\text{tot}}(x, \omega) \rangle + \frac{1}{2} \right). \quad (14)$$

In defining the total energy density, we have used the definition accounting for the energy of the polarizability of the matter. Furthermore, the media are assumed to be nonmagnetic. The magnitudes of the field fluctuations calculated from Eqs. (12) and (13) are continuous at interfaces as required by the boundary conditions, but the energy density in Eq. (14) can be discontinuous due to the effect of material polarizability.

Classically, EM forces are calculated using Maxwell's stress tensor [22, 23]. We apply the Maxwell's stress tensor in the form,

$$\vec{\mathbf{T}}(x, t) = \varepsilon_0 |n(x, \omega)|^2 \hat{E}(x, t)^2 \mathbf{y}\mathbf{y} + \frac{1}{\mu_0} \hat{B}(x, t)^2 \mathbf{z}\mathbf{z} - \hat{u}(x, t) \vec{\mathbf{I}}, \quad (15)$$

where the classical fields have been replaced by their quantum analogs and  $\vec{\mathbf{I}}$  is the unit dyadic presented in the Cartesian basis ( $\mathbf{x}, \mathbf{y}, \mathbf{z}$ ) as  $\vec{\mathbf{I}} = \mathbf{x}\mathbf{x} + \mathbf{y}\mathbf{y} + \mathbf{z}\mathbf{z}$ . The mechanical force density operator is given by [24, 25]

$$\hat{\mathbf{F}}(x, t) = \nabla \cdot \vec{\mathbf{T}}(x, t) - \frac{1}{c^2} \frac{\partial}{\partial t} \hat{\mathbf{S}}(x, t), \quad (16)$$

where  $\hat{\mathbf{S}}(x, t)$  is the Poynting vector operator and the last term in Eq. (16) gives the force density experienced by the EM field. In the steady state the expectation value of the last term is zero since the expectation value of the Poynting vector does not change in time. In one dimension the  $x$  component of the spectral force density expectation value then becomes

$$\begin{aligned} \langle \hat{F}_x(x, t) \rangle_\omega &= -\frac{\partial}{\partial x} \langle \hat{u}(x, t) \rangle_\omega \\ &= -\frac{\hbar\omega}{2} \left( \frac{\partial}{\partial x} \rho_{\text{tot}}(x, \omega) \right) - \hbar\omega \left( \frac{\partial}{\partial x} \rho_{\text{tot}}(x, \omega) \right) \\ &\quad \times \langle \hat{n}_{\text{tot}}(x, \omega) \rangle - \hbar\omega \rho_{\text{tot}}(x, \omega) \frac{\partial}{\partial x} \langle \hat{n}_{\text{tot}}(x, \omega) \rangle. \end{aligned} \quad (17)$$

The first term corresponds to the familiar zero-point Casimir force (ZCF) [26, 27], the second term is known as the thermal Casimir force (TCF) [28–30], and the last term arising from the changes in the total photon number is called a nonequilibrium Casimir force (NCF) since it disappears at thermal equilibrium when the derivative of the photon number is zero. The net force on any solid object extending from  $x_1$  to  $x_2$  can then be obtained as  $\langle \hat{\mathcal{F}}(t) \rangle_\omega / S = \int_{x_1}^{x_2} \langle \hat{F}_x(x, t) \rangle_\omega dx$ .

The net force can be also obtained by using the concept of EM pressure. The EM pressure along the  $x$  direction is obtained directly from the stress tensor as  $-\vec{\mathbf{T}}_{xx}$ , giving

$$\langle \hat{p}(x, t) \rangle_\omega = \hbar\omega \rho_{\text{tot}}(x, \omega) \left( \langle \hat{n}_{\text{tot}}(x, \omega) \rangle + \frac{1}{2} \right). \quad (18)$$

Therefore, the net force on an object extending from  $x_1$  to  $x_2$  can be obtained as  $\langle \hat{\mathcal{F}}(t) \rangle_\omega / S = \langle \hat{p}(x_1, t) \rangle_\omega - \langle \hat{p}(x_2, t) \rangle_\omega$ .

In small cavities the zero-point Casimir force usually dominates in the EM force. A possible measurement

setup in which the thermal and nonequilibrium contributions would be essential is, for example, the measurement of force exerted on a material slab placed in the middle of a symmetric cavity with boundaries at different temperatures. In this case, the densities of states on the different boundaries outside the slab would be equal [ $\rho_{\text{tot}}(x_1, \omega) = \rho_{\text{tot}}(x_2, \omega)$ ] due to the symmetry, and therefore, the zero-point Casimir contribution would cancel out. Then the spectral force on the slab simplifies to

$$\frac{\langle \hat{\mathcal{F}}(t) \rangle_\omega}{S} = \hbar\omega \rho_{\text{tot}}(x_1, \omega) \left( \langle \hat{n}_{\text{tot}}(x_1, \omega) \rangle - \langle \hat{n}_{\text{tot}}(x_2, \omega) \rangle \right). \quad (19)$$

Measuring forces on cavity walls also provides a possible scheme for determining the total EM LDOS and the total EM photon number inside the cavity. Knowing the source field photon numbers and measuring the forces (1) at equilibrium and (2) varying one of the reservoir temperatures, one can unambiguously solve the unknown LDOSs and the EM photon number inside the cavity. This is simplest in the nearly monochromatic case where the emissivity of the reservoirs are concentrated over a narrow spectrum, but it should also be possible in the more general case. The total EM LDOS and the total photon number can also be determined inside a cavity structure by separately measuring the electric and magnetic field LDOSs and photon numbers, which together determine the total field quantities as discussed in Sec. II C.

### III. RESULTS

#### A. Field temperatures

To investigate the physical implications of the concepts presented in Sec. II we study the properties of the effective field temperatures and the corresponding local densities of states in a vacuum cavity formed between two semi-infinite media with refractive indices  $n_1 = 1.5 + 0.3i$  and  $n_2 = 2.5 + 0.5i$ . The temperatures of the left and right thermal reservoirs formed by the semi-infinite media are  $T_1 = 400$  K and  $T_2 = 300$  K and the width of the vacuum gap is  $10 \mu\text{m}$ .

Figure 1 shows the LDOS for the electric, magnetic, and total EM fields and the corresponding effective field temperatures as a function of position. The electric LDOS in Fig. 1(a) oscillates in the vacuum and saturates to constant values in the lossy media far from the interfaces reflecting the formation of partial standing waves due to interference. The oscillation of the electric LDOS inside the cavity is strongest at resonant energies  $\hbar\omega = 0.056$  eV ( $\lambda = 22.1 \mu\text{m}$ ),  $\hbar\omega = 0.118$  eV ( $\lambda = 10.5 \mu\text{m}$ ), and  $\hbar\omega = 0.180$  eV ( $\lambda = 6.89 \mu\text{m}$ ). The oscillations in the electric LDOS manifest the Purcell effect and the related position-dependent strength of the field-matter coupling of particles placed in the cavity. The magnetic LDOS in Fig. 1(b) also oscillates inside the cavity. However, the positions of the peaks coincide with the minima of the electric LDOS in Fig. 1(a). In contrast to electric LDOS, the magnetic LDOS reaches its maximum values

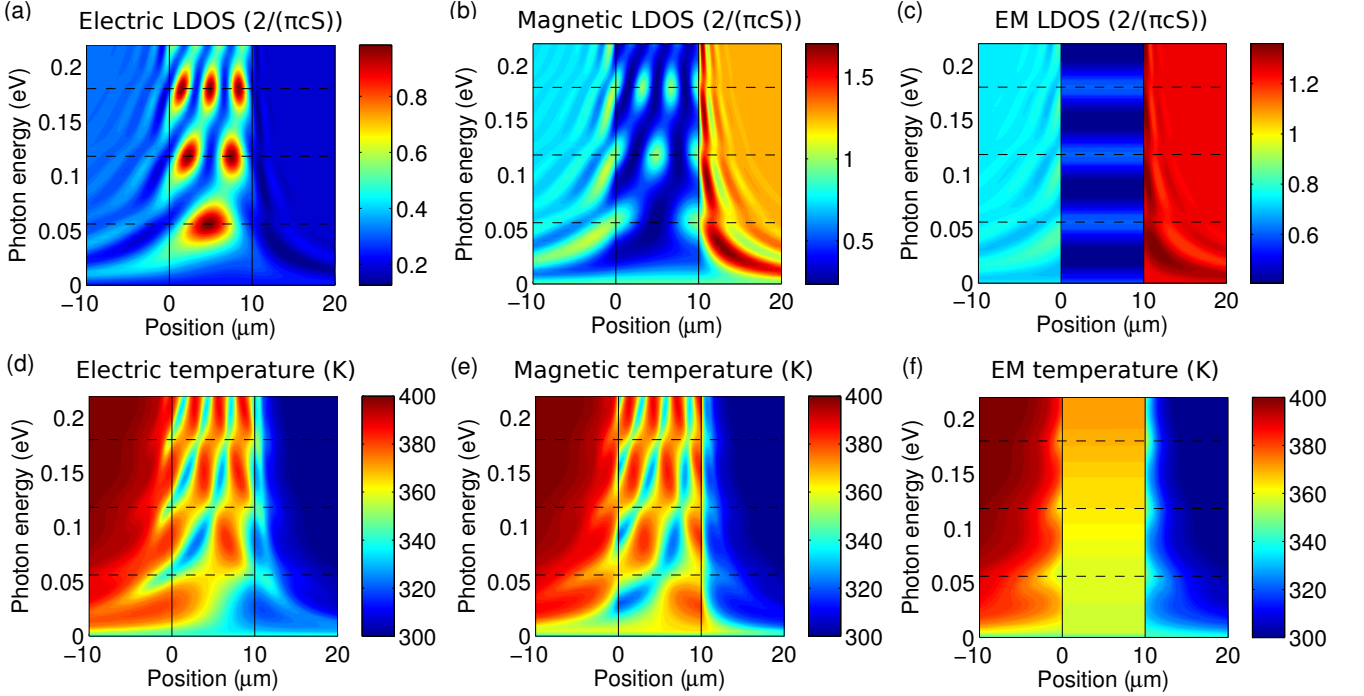


FIG. 1. (Color online) (a) Electric LDOS, (b) magnetic LDOS, (c) total EM LDOS, (d) electric field temperature, (e) magnetic field temperature, and (f) total field temperature in the vicinity of a vacuum gap separating lossy media with refractive indices  $n_1 = 1.5 + 0.3i$  and  $n_2 = 2.5 + 0.5i$  at temperatures 400 and 300 K. Solid lines denote the boundaries of the cavity and dashed lines denote resonant energies. The LDOSs are given in the units of  $2/(\pi c S)$ .

within the semi-infinite media due to the low finesse cavity and different dependence on the refractive index as can be seen in the latter form in Eq. (4) compared to the electric LDOS in Eq. (2). The total EM LDOS in Fig. 1(c) is constant with respect to position inside the cavity. This illustrates how the EM energy oscillates between its electric and magnetic forms in a way preserving the total energy. However, the total LDOS is position-dependent and oscillatory near interfaces inside the lossy media since the electric and magnetic LDOSs are not equal due to the bound states related to the material polarizability.

The effective field temperature defined using Eq. (10) is plotted for the electric field in Fig. 1(d). It has a strong position dependence and it oscillates both in the vacuum and inside the lossy media. The position dependence originates from the nonuniform coupling to the two thermal reservoirs. In the lossy media the oscillations are damped and the effective electric field temperature saturates to the reservoir temperature far from the interfaces. The characteristic distance for the damping of the oscillations depends on the photon energy and the material absorptivity and, in the selected example structure, it has a typical value of the order of  $10 \mu\text{m}$  increasing for smaller photon energies and decreasing for larger photon energies. Since the field-matter interaction takes place through the electric field, the local electric field temperature directly reveals the local material temperature re-

quired for having no net heat energy exchange between the field and matter making it an experimentally measurable quantity as discussed in Sec. II C. The magnetic field temperature is plotted in Fig. 1(e). It also has a strong position dependence, but the peaks are located at different positions when compared to the electric field temperature in Fig. 1(d).

The total EM field temperature in Fig. 1(f) is constant with respect to position inside the cavity as the total EM LDOS in Fig. 1(c). The position independence of the total field temperature follows from the position independence of the total EM photon number in the vacuum as discussed in Sec. II. In contrast to the electric and magnetic field temperatures in Figs. 1(d) and 1(e), the changes of the total EM field temperature and photon number near interfaces are always monotonic with respect to position, which is an expected result for the photon number of the total EM field.

## B. Electromagnetic forces

Next we study the Casimir force densities in a lossy cavity filled with material having refractive index  $n_c = 1.1 + 0.1i$ . As before, the cavity width is  $10 \mu\text{m}$  and the left and right cavity boundaries have refractive indices  $n_1 = 1.5 + 0.3i$  and  $n_2 = 2.5 + 0.5i$  and temperatures 400 and 300 K. In contrast to the vacuum cavity case, the lossy cavity medium acts as an additional field source emitting photons. In this work, we calculate the temper-

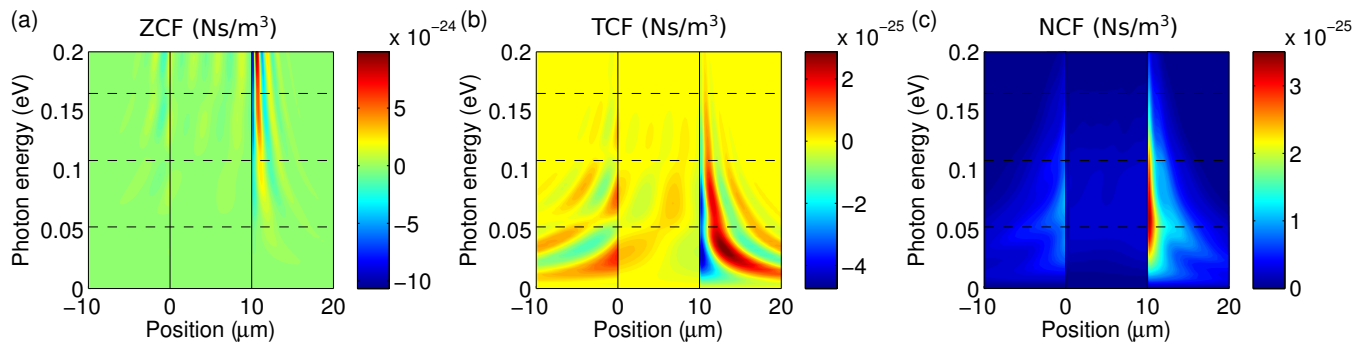


FIG. 2. (Color online) (a) The zero-point, (b) thermal, and (c) nonequilibrium Casimir force contributions of the spectral force density in the case of a 10- $\mu\text{m}$  wide lossy cavity with refractive index  $n_c = 1.1 + 0.1i$ . The left and right cavity boundaries have refractive indices  $n_1 = 1.5 + 0.3i$  and  $n_2 = 2.5 + 0.5i$  and temperatures 400 and 300 K. Solid lines denote the boundaries of the cavity and dashed lines denote resonant energies.

ature of the lossy cavity medium self-consistently so that the photon emission equals absorption at every point, i.e., the net emission rate in Eq. (11) is zero. This also means that other heat conduction mechanisms than radiation are neglected.

The force density contributions calculated by using Eq. (17) are plotted in Fig. 2 as a function of the position and photon energy. Since the refractive index forms step functions at the interfaces, it follows from definitions (8) and (9) that the total EM LDOS and the total EM photon number are also discontinuous so that the force density contributions contain delta functions at the interfaces. This can not be seen in the figures and it will give an additional contribution when integrating the total force. The spectral component of the zero-point Casimir force is shown in Fig. 2(a), the thermal Casimir force in Fig. 2(b), and the nonequilibrium Casimir force in Fig. 2(c). The zero-point Casimir force dominates especially in the case of high frequencies except close to its zeros where the thermal and nonequilibrium contributions become important. The thermal and nonequilibrium contributions decay at high frequencies due to the smaller thermal excitation of the high energy states. In contrast, the zero-point Casimir force does not decay but increases with frequency since the materials are assumed to be nondispersive in the studied frequency range. One can also see that the zero-point and thermal Casimir contributions both obtain positive and negative values corresponding to forces to the left and right depending on the position and photon energy. In contrast, the nonequilibrium Casimir force is always positive since the derivative of the photon number is negative in Eq. (17) because the total photon number monotonically decreases towards the colder medium. The direction and magnitude of the total force density depends on the value of the integral when the spectral force density is integrated over the frequency axis. The observable total force exerted on a volume is the sum of the three force density components integrated over the volume.

To learn more on the EM pressure under conditions where the well-known zero-point Casimir force vanishes we study the force exerted on lossy and lossless material slabs placed in the middle of a symmetric vacuum cavity. In the case of a slab in the middle of a symmetric cavity, the force is nonzero only for setups that are not under thermal equilibrium since the zero-point Casimir contribution to the force cancels resulting in the force in Eq. (19). In contrast to the previous geometry, the refractive indices of cavity boundaries are equal  $n_1 = n_2 = 2.5 + 0.5i$ , but the left and right reservoir temperatures are 400 and 300 K as before.

The total spectral force experienced by the lossy slab with refractive index  $n_{\text{slab}} = 1.5 + 0.3i$  is plotted in Fig. 3(a) as a function of the slab width and photon energy. The force is always directed towards the colder material. In the limit of zero slab width, the force goes to zero since the volume of the interacting slab material disappears. When the slab width is increased, also the force increases. However, the force disappears for low and high frequencies as the photon energy  $\hbar\omega$  or the photon probability given by the Bose-Einstein distribution becomes zero. Also note that the force becomes zero for all slab widths and photon energies if the left and right reservoir temperatures are equal.

The total force experienced by the lossless slab with real refractive index  $n_{\text{slab}} = 1.5$  is plotted in Fig. 3(b). Comparison with the case of a lossy slab in Fig. 3(a) shows that the force strongly depends on losses. The force on a lossless slab can clearly obtain negative values for some frequencies and slab widths indicating that the force is unexpectedly towards the medium at higher temperature while the energy flow according to the Poynting vector is towards the medium at lower temperature. This is called optical pulling force [31] and it is expected to be possible because of the combined effect of cavity resonances and the proportionally larger contribution of the low energy photons of the lower temperature thermal reservoir.



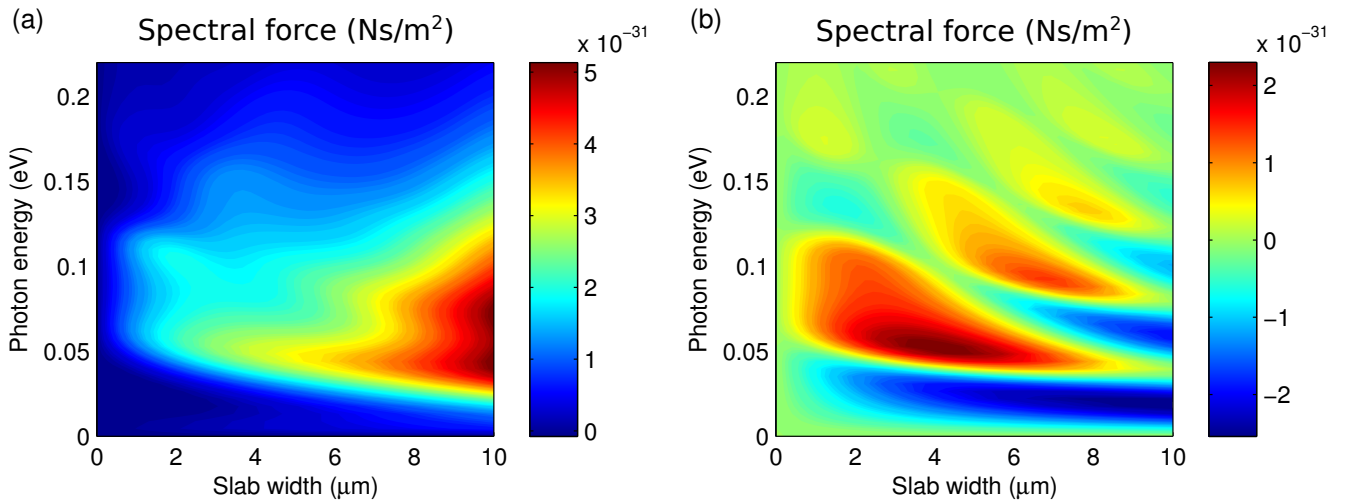


FIG. 3. (Color online) (a) The spectral force exerted on a lossy material slab with refractive index  $n_{\text{slab}} = 1.5 + 0.3i$  inside the  $10\text{-}\mu\text{m}$  wide vacuum cavity. (b) The spectral force in the case of a lossless material slab with refractive index  $n_{\text{slab}} = 1.5$ . The left and right cavity boundaries have equal refractive indices  $n_1 = n_2 = 2.5 + 0.5i$  and temperatures 400 and 300 K. The center of the slab is positioned in the middle of the cavity.

#### IV. CONCLUSIONS

The quantization approach we recently introduced to define position-dependent ladder operators to describe the quantized electric field and light-matter interactions was extended to also describe the quantization of the magnetic and total EM fields. The quantization is based on defining electric, magnetic, and total EM photon ladder operators that by definition obey the canonical commutation relations. The previous electric-field-based quantization was only able to describe the electric field photon number and local energy balance, whereas the generalized approach also allows consistent quantum optical description of the magnetic and total EM field photon numbers, energy balance of magnetic interactions, radiation pressure, and EM forces in lossy and dispersive structures. One additional strength of the formalism is that formulas involving photon-number expectation values are expected to generalize to fields with any kind of quantum statistics, such as single photon and laser fields.

We have studied the energy flow and induced EM forces in cavity structures with cavity walls at different temperatures. Our results show that the electric and

magnetic field operators and temperatures are generally position dependent under nonequilibrium conditions due to being defined in terms of the position-dependent noise fields generating them. However, the photon number associated with the total EM field is always constant in lossless media as one might also intuitively expect from a quantum number describing the energy density of the total EM field. Furthermore, the direction of the EM force in the cavity was shown to be position dependent producing optical pulling and pushing forces at different cavity positions.

We expect that our model will give insight in studying the optical energy transfer in nanodevices as well as modeling optomechanical devices. In addition, extending the formalism to quantum systems that are not limited to thermal fields could possibly enable a versatile approach to model various quantum optical experiments.

#### ACKNOWLEDGMENTS

This work has in part been funded by the Academy of Finland and the Aalto Energy Efficiency Research Programme.

- 
- [1] L. Knöll, W. Vogel, and D.-G. Welsch, *Phys. Rev. A* **43**, 543 (1991).
  - [2] L. Allen and S. Stenholm, *Opt. Commun.* **93**, 253 (1992).
  - [3] B. Huttner and S. M. Barnett, *Phys. Rev. A* **46**, 4306 (1992).
  - [4] R. Barnett, S. M. Matloob and R. Loudon, *J. Mod. Opt.* **42**, 1165 (1995).
  - [5] R. Matloob, R. Loudon, S. M. Barnett, and J. Jeffers, *Phys. Rev. A* **52**, 4823 (1995).
  - [6] R. Matloob and R. Loudon, *Phys. Rev. A* **53**, 4567 (1996).
  - [7] M. G. Raymer and C. J. McKinstrie, *Phys. Rev. A* **88**, 043819 (2013).
  - [8] S. M. Barnett, C. R. Gilson, B. Huttner, and N. Imoto, *Phys. Rev. Lett.* **77**, 1739 (1996).
  - [9] M. Ueda and N. Imoto, *Phys. Rev. A* **50**, 89 (1994).
  - [10] A. Aiello, *Phys. Rev. A* **62**, 063813 (2000).
  - [11] O. Di Stefano, S. Savasta, and R. Girlanda, *Phys. Rev. A* **61**, 023803 (2000).
  - [12] M. Partanen, T. Häyrynen, J. Oksanen, and J. Tulkki,

- Phys. Rev. A **89**, 033831 (2014).
- [13] M. Partanen, T. Häyrynen, J. Oksanen, and J. Tulkki, in *Proc. SPIE 9136, Nonlinear Optics and Its Applications VIII; and Quantum Optics III*, 91362B (SPIE, 2014).
  - [14] S. Scheel, L. Knöll, and D.-G. Welsch, Phys. Rev. A **58**, 700 (1998).
  - [15] T. Gruner and D.-G. Welsch, Phys. Rev. A **54**, 1661 (1996).
  - [16] K. Joulain, R. Carminati, J.-P. Mulet, and J.-J. Greffet, Phys. Rev. B **68**, 245405 (2003).
  - [17] C. F. Bohren and D. R. Huffman, *Absorption and scattering of light by small particles* (Wiley, Chichester, UK, 1998).
  - [18] S. Tumanski, Meas. Sci. Technol. **18**, R31 (2007).
  - [19] J. P. Pendry, A. J. Holden, D. J. Robbins, and W. J. Stewart, IEEE Trans. Microw. Theory Tech. **47**, 2075 (1999).
  - [20] J. Lazar, O. Cip, J. Oulehla, P. Pokorný, A. Fejfar, and J. Stuchlik, in *Proc. SPIE 8306, Photonics, Devices, and Systems V*, 830607 (SPIE, 2011).
  - [21] M. Hola, J. Hrabina, O. Cip, A. Fejfar, J. Stuchlik, J. Kocka, J. Oulehla, and J. Lazar, in *Nanocon 2013. 5th International Conference* (2013) <http://hdl.handle.net/11104/0225472>.
  - [22] J. D. Jackson, *Classical electrodynamics* (Wiley, New York, 1999).
  - [23] L. D. Landau, E. M. Lifshitz, and L. P. Pitaevskii, *Electrodynamics of continuous media*, 2nd ed. (Pergamon, Oxford, 1984).
  - [24] L. Novotny and B. Hecht, *Principles of nano-optics* (Cambridge University Press, Cambridge, 2006).
  - [25] M. Maggiore, *A Modern Introduction to Quantum Field Theory* (Oxford University Press, Oxford, 2005).
  - [26] A. W. Rodriguez, F. Capasso, and S. G. Johnson, Nature Photonics **5**, 211 (2011).
  - [27] M. Antezza, L. P. Pitaevskii, S. Stringari, and V. B. Svetovoy, Phys. Rev. A **77**, 022901 (2008).
  - [28] R. Passante and S. Spagnolo, Phys. Rev. A **76**, 042112 (2007).
  - [29] A. O. Sushkov, W. J. Kim, D. A. R. Dalvit, and S. K. Lamoreaux, Nature Physics **7**, 230 (2011).
  - [30] G. L. Klimchitskaya, U. Mohideen, and V. M. Mostepanenko, J. Phys. A **41**, 432001 (2008).
  - [31] J. Chen, J. Ng, Z. Lin, and C. T. Chan, Nature Photonics **5**, 531 (2011).